

Shape Design Optimization of Unimorph Piezoelectric Cantilever Energy Harvester

Rouhollah Hosseini*, Maryam Nouri

Young Researchers and Elite Club, South Tehran Branch, Islamic Azad University, Tehran, Iran

Received: 13 Oct. 2016 , Accepted: 28 Dec. 2016

Abstract

The most promising method for micro scale energy scavenging is via vibration energy harvesting which converts mechanical energy to electrical energy. Using piezoelectric cantilevers is the most common method for vibration energy harvesting. Changing the shape of the cantilevers can lead to changing the generated output voltage and power. In this work vibration energy harvesting via piezoelectric resonant unimorph cantilevers is studied and new design for obtaining more efficient piezoelectric energy harvester is suggested. This study provides comprehensive analysis of the output voltage relationships and deducing a considerable precise rule of thumb for calculating resonance frequency in cantilever-type unimorph piezoelectric energy harvesters using Rayleigh method. The analytical formula, is then analyzed and verified by FEM simulation in ABAQUS. The analytical data was found to be very close to simulation data. A key finding is that among all the unimorph trapezoidal V-shaped cantilever beams with uniform thickness, the triangular tapered cantilever, can lead to highest resonance frequency and by increasing the ratio of the trapezoidal bases, the resonance frequency decreases. These new findings provide guidelines on system parameters that can be manipulated for more efficient performance in different ambient source conditions.

Keywords: Vibration energy harvesting, Unimorph Piezoelectric vibrator, Trapezoidal V-shaped cantilever, Triangular beam, Resonant frequency

1. Introduction

The conversion of ambient energy in the environment surroundings into electrical energy is called energy harvesting or energy scavenging. During the past decade, energy harvesting from mechanical vibrations of ambient environments has attracted the attention of many researchers due to the ever increasing desire to produce wireless and portable electronics with extended life. While sensors and wireless electronic equipment to support pervasive computing are becoming more prevalent, delivering power to the

wireless sensor networks is difficult and remains a challenge. Mechanical vibrations are abundant and ubiquitous in environment, and they provide no limitations in their applications on cloudy days or at nights. The prevalent mechanisms for vibration energy harvesting are: using electrostatic devices, electromagnetic field and utilizing piezoelectric materials. Piezoelectric based material's flexibility in volume and size has led to the development of micro generators, that they are utilized in places where other sources of energy are not readily available [1].

Vibration energy harvesting with piezoelectric material can currently generate up to 300 microwatts

* Corresponding Author. Tel.: +982177105105
Email Address: r.hosseini.mech@gmail.com

per cubic centimeter, making it an attractive method of powering low-power electronics [2]. Compared to other structural forms of beams, a cantilever has the maximum deformation under the same conditions. The larger deflection leads to higher strain and hence more output power. Therefore the vast majority of piezoelectric vibration power scavenging devices use a cantilever structure [3-6]. A cantilever-type power scavenger has been intensively studied and a tapered one has been found to be the optimum design [7-9], because it ensures a large constant and more uniform distribution of strain in the piezoelectric layer resulting in higher power output in comparison to the rectangular beam with the length and width equal to the height and base of the corresponding tapered cantilever beam.

A piezoelectric unimorph cantilever structure includes one inactive (substrate) and one active (piezoelectric) layer, whereas a bimorph cantilever has one inactive layer, but two active layers. In order to analyze and calculate the resonance frequency of unimorph trapezoidal V-shaped cantilever beams (in special case triangular cantilevers), a significant and simple analytical formula using Rayleigh method is derived and then the optimization method for adjusting (enhancing or lowering) the resonance frequency with this formula is used. In special case that piezoelectric layer thickness is negligible and trapezoid becomes a triangle, the resonance frequency formulation for a simple triangular cantilever is formulated that is in accordance with that extracted in [10-12]. The extracted analytical formula and the results, are verified by FEM simulation in ABAQUS 14.1 software, and presents a strong potential to be used in the design and optimization of unimorph trapezoidal V-shaped cantilever piezoelectric energy harvesters. It is noteworthy that a cantilever beam has many different modes of vibration in different resonance frequencies. The first mode of vibration in the fundamental mode and has the lowest resonant frequency. This fundamental mode of vibration typically provides the most deflection and hence output voltage and power. Accordingly, power scavengers are generally designed to operate in the fundamental resonance frequency [13, 14].

Then, under the influence of base excitation, estimation of voltage response for rectangular and tapered unimorph piezoelectric cantilever beam is done. Because of the lack of analytical solution for a triangular tapered cantilever, the numerical solution is done and the result is compared with the nearest exponentially tapered cantilever shape that has the analytical solution. Analytical formulas in forced vibration analysis are validated by finite element

simulation. Studies are carried out using MATLAB, ABAQUS and MATHEMATICA software.

This paper presents work on improving unimorph piezoelectric vibration energy harvesters based on the structural modifications. A new design for a unimorph cantilever-type piezoelectric energy harvester is proposed and the main focus of this paper is to study the resonance frequency and output voltage of the proposed design in piezoelectric mechanical energy harvester.

2. Modal analysis

The structure of unimorph piezoelectric rectangular cantilever is shown in Figure 1. In Figure 1, l is the length, w is the width, ρ_s and ρ_p are the substrate and piezoelectric density, t_s and t_p are the substrate and piezoelectric thickness, and E_s and E_p are the Young's modulus for substrate and piezoelectric layers, respectively. Also the total cross-sectional area moment of inertia is \bar{I}_z .

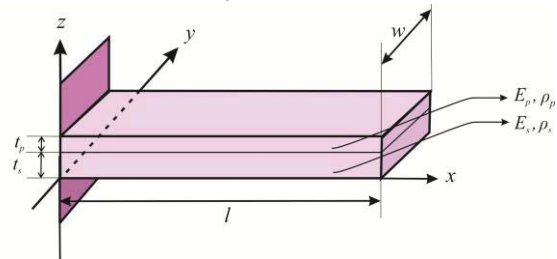


Figure 1 Schematic of a simple unimorph cantilever beam

For beam cross-sections that are not symmetric about the y-axis with regard to either geometry or the variation of elasticity modulus (E), a convenient method for treating bending problems is provided by the concept of the transformed section. If we choose a certain value of E as a reference value and call it E_{ref} , then we can define a transformed section and transformed width nw , where $n = E_s / E_p$. In this case we assume that $E_{ref} = E_p$. The line of action of an axial force producing purely axial deformation, passes through the centroid of the transformed section. In the case of bending without any axial force, the neutral axis passes through this point. In this case we assume that the location of the effective centroid is determined by h (Figure 2 and Figure 3) [15].

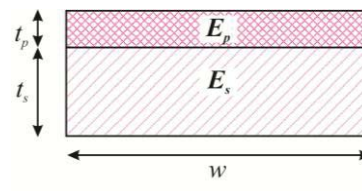


Figure 2 cross section of unimorph cantilever

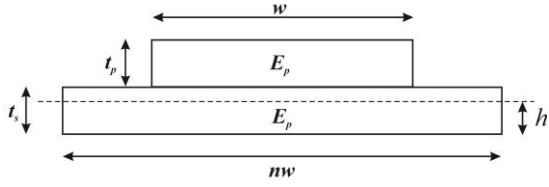


Figure 3 transformed section of unimorph cantilever

h is applied for determination of the neutral axis location:

$$h = \frac{nt_s^2 + 2t_s t_p + t_p^2}{2nt_s + 2t_p} \quad (7)$$

The total cross-sectional area moment of inertia can be expressed as:

$$\bar{I}_z = \frac{nw t_s^3}{12} + nwt_s \left(h - \frac{t_s}{2}\right)^2 + \frac{w t_p^3}{12} + w t_p \left(\frac{t_p}{2} + t_s - h\right)^2 \quad (8)$$

When applying a normal force F at the free end of the cantilever, the deflection function along the length direction can be expressed as:

$$z(x) = \frac{Fx^2(3l-x)}{6E_p I} = Kx^2(3l-x) \quad (9)$$

where K is a constant. The deflection function of (9) can be used as the mode shape, for extracting the resonant behavior of a unimorph cantilever beam with an arbitrary form and width function $w(x)$ [16]. So the vibration displacement at each position is:

$$z(x, \tau) = Kx^2(3l-x)\sin(\omega\tau + \psi) \quad (10)$$

where K and ψ are constants, $\omega=2\pi f$ is the angular frequency and τ is the time.

The kinetic energy of the vibrant unimorph cantilever beam can be written as [17]:

$$\begin{aligned} T &= \frac{1}{2} \int_0^l (\rho_s t_s + \rho_p t_p) w(x) dx \left(\frac{\partial z}{\partial \tau}\right)^2 \\ &= \int_0^l \frac{1}{2} (\rho_s t_s + \rho_p t_p) w(x) \left[\omega Kx^2(3l-x)\cos(\omega\tau + \alpha)\right]^2 dx \end{aligned} \quad (11)$$

$$f(w(x)) = \frac{\omega}{2\pi} = \frac{\sqrt{3}}{\pi} \sqrt{\frac{E_s(t_s-h)^3 + E_s h^3 + E_p(t_s+t_p-h)^3 - E_p(t_s-h)^3}{\rho_s t_s + \rho_p t_p}} \sqrt{\frac{\int_0^l w(x)(l-x)^2 dx}{\int_0^l w(x)x^4(3l-x)^2 dx}} \quad (15)$$

The maximum kinetic energy of the vibrant unimorph cantilever is obtained as:

$$T_{\max} = \frac{1}{2} (\rho_s t_s + \rho_p t_p) \omega^2 K^2 \int_0^l w(x)x^4(3l-x)^2 dx \quad (12)$$

The potential energy of the system can be written as [17]:

$$\begin{aligned} V &= \frac{1}{2} \iiint_V \sigma_{xx} \varepsilon_{xx} dV = \\ &= \frac{1}{2} \int_0^l \int_0^{w(x)} \int_{-h}^{t_s+t_p-h} \sigma_{xx} \varepsilon_{xx} dV \\ &= \int_0^l \frac{w(x)}{2} \left(\frac{\partial^2 z}{\partial x^2}\right)^2 \left[\frac{E_s}{3}(t_s-h)^3 + \frac{E_s}{3}h^3 + \frac{E_p}{3}(t_s+t_p-h)^3 - \frac{E_p}{3}(t_s-h)^3 \right] dx \\ &= 18K^2 \sin^2(\omega\tau + \alpha) \left[\frac{E_s}{3}(t_s-h)^3 + \frac{E_s}{3}h^3 + \frac{E_p}{3}(t_s+t_p-h)^3 - \frac{E_p}{3}(t_s-h)^3 \right] \int_0^l w(x)(l-x)^2 dx \end{aligned} \quad (13)$$

So the maximum potential energy of the unimorph cantilever is:

$$V_{\max} = 18K^2 \left[\frac{E_s}{3}(t_s-h)^3 + \frac{E_s}{3}h^3 + \frac{E_p}{3}(t_s+t_p-h)^3 - \frac{E_p}{3}(t_s-h)^3 \right] \int_0^l w(x)(l-x)^2 dx \quad (14)$$

According to conservation law of mechanical energy, the resonant frequency can be obtained as [14, 18]:

In the particular case, for a rectangular cantilever with length l_1 , width w_1 , thicknesses t_s and t_p , mass densities ρ_s and ρ_p and Young's modulus E_s and E_p , the deduced resonant frequency is as:

$$f_{rect} = \frac{\sqrt{385}}{11\pi l_1^2} \sqrt{\frac{(E_s(t_s - h)^3 + E_s h^3 + E_p(t_s + t_p - h)^3 - E_p(t_s - h)^3)}{\rho_s t_s + \rho_p t_p}} \quad (16)$$

As mentioned in [13], a typical trapezoidal V-shaped cantilever is the result of difference between one triangular tapered cantilever and one trapezoidal tapered cantilever, with same thickness, with lengths l_0 and l_1 , and with widths w_0 and w_1 respectively (Figure 4(a)). Because of the mirror symmetry of V-shaped cantilever, it is only necessary to analyze half of the geometry, which is a quadrilateral cantilever (Figure 4(b)).

Evidently for the quadrilateral cantilever beam, the width is a piecewise-continuous function of x , that is:

$$w(x) = \begin{cases} \frac{w_1}{2} \left(1 - \frac{x}{l_1 + l_2}\right) - \frac{w_0}{2} \left(1 - \frac{x}{l_0}\right), & x \in [0, l_0] \\ \frac{w_1}{2} \left(1 - \frac{x}{l_1 + l_2}\right), & x \in [l_0, l_1] \end{cases} \quad (17)$$

For simplifying calculations, it is reasonable to define the width ratios a and b , and the length ratio c of the trapezoidal V-shaped cantilever beam:

$$a = \frac{w_2}{w_1}, b = \frac{w_0}{w_1}, c = \frac{l_0}{l_1} \quad (18)$$

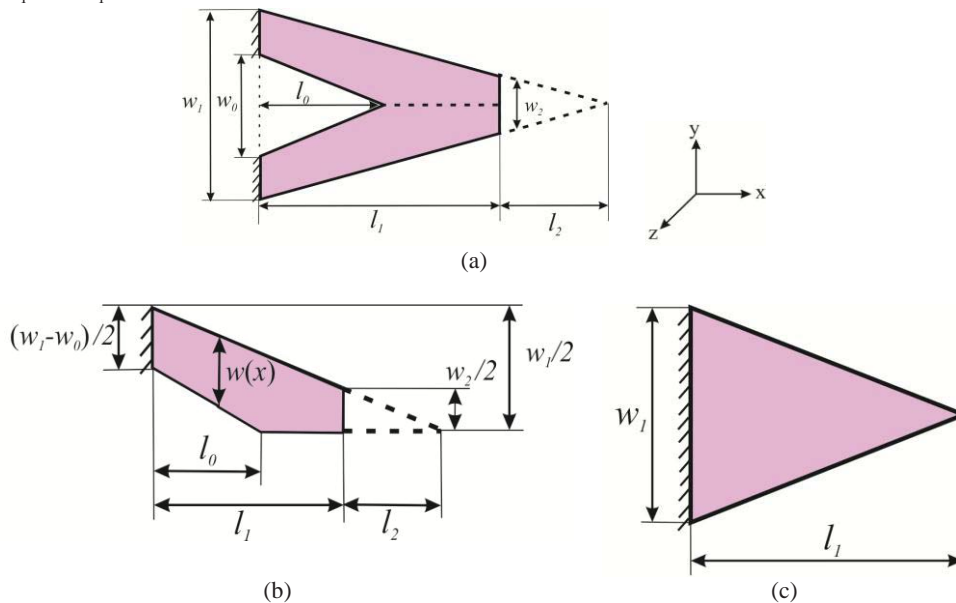


Figure 4 Shape and dimension of (a) trapezoidal V-shaped cantilever beam (b) half of the trapezoidal V-shaped cantilever beam (c) triangular tapered cantilever beam

Substituting (17) and (18) into (15), the resonant frequency formula of the trapezoidal cantilever beam is obtained:

$$f(w(x)) = \frac{\sqrt{70}}{\pi l_1^2} \sqrt{\frac{(E_s t_s - h^3 + E_s h^3 + E_p t_s + t_p - h^3 - E_p t_s - h^3)}{\rho_s t_s + \rho_p t_p} \frac{3 + a - 6bc + 4bc^2 - bc^3}{49 + 250a - 84bc^5 + 40bc^6 - 5bc^7}} \quad (19)$$

In order to represent the relationship between the resonant frequency and the ratios a , b and c , a characteristic function in terms of a , b and c can be defined as mentioned in [11] and [13]:

$$g(a, b, c) = \sqrt{\frac{3 + a - 6bc + 4bc^2 - bc^3}{49 + 250a - 84bc^5 + 40bc^6 - 5bc^7}} \quad (20)$$

$a \in [0, 1], b \in [0, 1], c \in [0, 1]$

Hence, the resonant frequency of unimorph trapezoidal V-shaped cantilever beam is:

$$f(w(x)) = \frac{\sqrt{70}}{\pi l_1^2} \sqrt{\frac{(E_s t_s - h^3 + E_s h^3 + E_p t_s + t_p - h^3 - E_p t_s - h^3)}{\rho_s t_s + \rho_p t_p} g(a, b, c)} \quad (21)$$

For a unimorph triangular tapered cantilever, $a=0$ and the resonant frequency is:

$$f(w(x)) = \frac{\sqrt{70}}{\pi l_1^2} \sqrt{\frac{E_s t_s - h^3 + E_s h^3 + E_p t_s + t_p - h^3 - E_p t_s - h^3}{\rho_s t_s + \rho_p t_p}} g(a=0, b, c) \quad (22)$$

In other words, characteristic function will be summarized as:

$$g(b, c) = \sqrt{\frac{3 - 6bc + 4bc^2 - bc^3}{49 - 84bc^5 + 40bc^6 - 5bc^7}} \quad (23)$$

$$b \in [0, 1], c \in [0, 1]$$

In the special case that $t_p=0$ and $a=0$, the resonant frequency formulation for a simple triangular cantilever beam is obtained that is in accordance with that extracted in [12].

As shown in Figure 5, $g(a, b, c)$ reaches the maximum value $\frac{\sqrt{3}}{7} \approx 0.2474$, when $a=0$ and $c=0$ or $c=1$ or $b=0$. That means if $l_0=0$ or $l_0=l_2$ or $w_0=0$, unimorph trapezoidal V-shaped cantilever achieves highest resonant frequency. For $w_2=0$ and $l_0=0$ or $w_0=0$, the unimorph trapezoidal V-shaped cantilever beam turns into a unimorph triangular tapered cantilever beam as shown in Figure 4(c). When $w_2=0$ and $l_0=l_1$, the unimorph V-shaped cantilever turns into two side by side unimorph tapered cantilever beams, though, this particular uncommon form is difficult to accomplish. Therefore, unimorph tapered cantilever

beam that is easy for micro-fabrication and is a special kind of unimorph V-shaped cantilever beam, can reach the maximum resonant frequency. In other words, it has the highest sensitivity. It is notable that the behavior of $g(a, b, c)$ in Figure 5 is such as that obtained in [18].

3. Electrical potential response of a unimorph piezoelectric cantilever

Because of the low thickness of the beam, Euler-Bernoulli theory is considered in deriving the mathematical modelling of the structure. The governing equation of motion for a beam embedded by a single piezoelectric layer under the influence of base excitation is as follows [19]:

$$\frac{\partial^2 M(x, t)}{\partial x^2} + \frac{\partial^2}{\partial x^2} \left(C_s I(x) \frac{\partial^3 z(x, t)}{\partial x^2 \partial t} \right) + C_a \frac{\partial z(x, t)}{\partial t} + m(x) \frac{\partial^2 z(x, t)}{\partial t^2} = -[m(x) + M_t \delta(x - L)] \frac{\partial^2 z_b(x, t)}{\partial t^2} \quad (24)$$

where $M(x, t)$ is the internal moment, $z(x, t)$ is the transverse displacement of the neutral axis, $z_b(x, t)$ is the base excitation displacement, C_s and C_a are equivalent strain rate and viscous air damping coefficient, $I(x)$ is the area moment of inertia, $m(x)$ is the mass per unit length of the beam and M_t is the tip mass. For this structure, the boundary conditions of the system are described in Eq.(25) i.e. the cantilever is fixed at $x=0$ and attached to a tip mass at the other end [3].

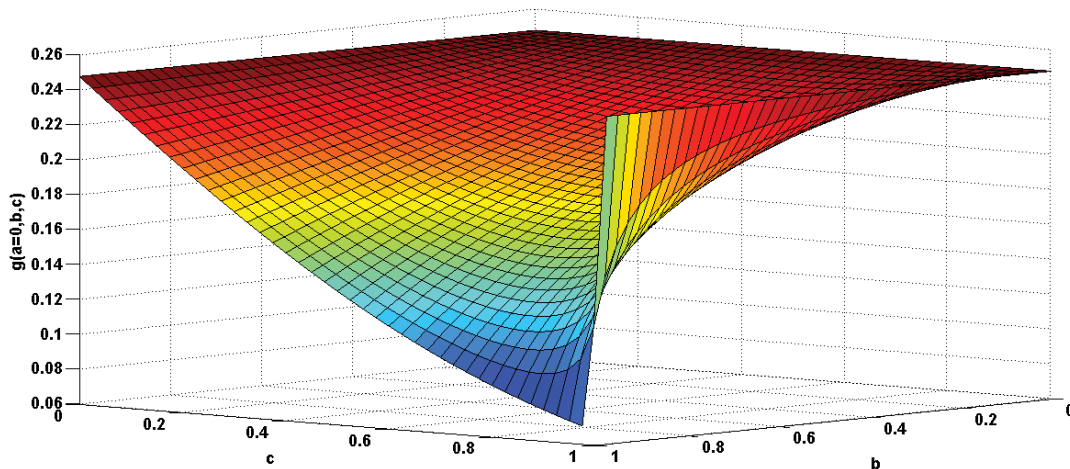


Figure 5 The function image of $g(a=0, b, c)$

$$z(0,t) = 0, \frac{\partial z(x,t)}{\partial x} = 0, \quad (25)$$

$$EI \frac{\partial^3 z(x,t)}{\partial x^3} = M_t \frac{\partial^2 z(x,t)}{\partial t^2},$$

$$EI \frac{\partial^2 z(x,t)}{\partial x^2} = I_t \frac{\partial^3 z(x,t)}{\partial x \partial t^2}$$

where I_t is the rotary inertia of the tip mass. Here it is assumed to neglect the tip mass.

As the unimorph cantilever, consists of two layers with different materials, m can be written as:

$$m = w(\rho_s t_s + \rho_p t_p) \quad (26)$$

where w is the width, t is the thickness and ρ is the density. Also the subscripts s and p , are for substrate and piezoelectric layers, respectively. Here, the width of the piezoelectric layer is assumed to be the same as the width of the substrate layer, denoted by w . The internal moment $M(x,t)$, can be written as:

$$M(x,t) = - \int_{-(t_s/2)}^{(t_s/2)} \sigma_1^s w y dy - \int_{(t_s/2)}^{(t_s/2)+t_p} \sigma_1^p w y dy \quad (27)$$

Using the constitutive equation of piezoelectric and isotropic material, the stress terms in the relation (27) can be written as follows:

$$\sigma_1^s = E_s \varepsilon_1^s(x,t) \quad (28)$$

$$\sigma_1^p = E_p (\varepsilon_1^p(x,t) - d_{31} E_3(t)) \quad (29)$$

where σ is the normal stress in x direction, ε is the mechanical strain, d_{31} is the piezoelectric strain constant, and E_3 is the applied electrical field. E_3 can be written in terms of voltage $v(t)$ as below:

$$E_3(t) = -v(t) / h_p \quad (30)$$

The bending strain, ε at any level, z from the neutral axis can be expressed as below:

$$\varepsilon_1 = -y \frac{\partial^2 z_{rel}(x,t)}{\partial x^2} \quad (31)$$

Employing equations, (28), (29) and (31) into Eq. (27), one may obtain:

$$M(x,t) = EI(x) \frac{\partial^2 z_{rel}(x,t)}{\partial x^2} + \eta(x)v(t) \quad (32)$$

where:

$$\eta(x) = -\frac{1}{2} E_p w(x) d_{31} (t_p + t_s) \quad (33)$$

Using Heaviside step function, the internal moment can be written as:

$$M(x,t) = EI(x) \frac{\partial^2 z_{rel}(x,t)}{\partial x^2} + \eta(x)v(t)[He(x) - He(x-l)] \quad (34)$$

where l is the length of the beam and piezoelectric layer covers all of this length. Employing eq.(34) into eq.(24) yields:

$$\frac{\partial^2}{\partial x^2} \left[EI(x) \frac{\partial^2 z_{rel}(x,t)}{\partial x^2} \right] + \frac{\partial^2}{\partial x^2} \left[C_s I(x) \frac{\partial^3 z_{rel}(x,t)}{\partial x^2 \partial t} \right] + C_a \frac{\partial z_{rel}(x,t)}{\partial t} + m(x) \frac{\partial^2 z_{rel}(x,t)}{\partial t^2} \quad (35)$$

$$+ \frac{\partial^2}{\partial x^2} \left[\eta(x)v(t) \left[\frac{d\delta(x)}{dx} - \frac{d\delta(x-l)}{dx} \right] \right] = - (m(x) + M_t \delta(x-l)) \frac{\partial^2 z_b(x,t)}{\partial t^2}$$

The constitutive equation of piezoelectric materials that relates the electrical and mechanical terms is given by:

$$D_3(x,t) = d_{31} \sigma_1(x,t) + \varepsilon_{33}^T E_3(t) \quad (36)$$

Here $D_3(x,t)$ is the electrical displacement, $\sigma_1(x,t)$ is the normal stress in x direction and ε_{33}^T is the permittivity at constant stress. The permittivity at constant strain ε_{33}^S , replaces the permittivity component through $\varepsilon_{33}^S = \varepsilon_{33}^T - d_{31} E_3$. Thus eq. (36) can be rewritten as:

$$D_3(x,t) = -d_{31} E_p \left(\frac{t_s}{2} + t_p \right) \frac{\partial^2 z_{rel}(x,t)}{\partial x^2} - \varepsilon_{33}^S \frac{v(t)}{t_p} \quad (37)$$

Integrating the electrical displacement over the piezoelectric area leads to generated electric charge in piezoelectric layer, $q(t)$, as below :

$$q(t) = \int \vec{D}_3 \cdot \vec{n} dA = - \int_{x=0}^{x=l} \left(d_{31} \left(\frac{t_s}{2} + t_p \right) E_p w(x) \frac{\partial^2 z_{rel}(x,t)}{\partial x^2} + \varepsilon_{33}^S w(x) \frac{v(t)}{t_p} \right) dx \quad (38)$$

where \vec{n} is unit outward normal and \vec{D} is the vector of electric displacement. Value of the current, $i(t)$ is obtained by differentiating electrical charge over time. Therefore, the voltage across the resistive load can be obtained as follows:

$$v(t) = R_L i(t) = -R_L \left[\int_{x=0}^{x=l} \left(d_{31} \left(\frac{t_s}{2} + t_p \right) E_p w(x) \frac{\partial^3 z_{rel}(x,t)}{\partial x^2 \partial t} \right) dx + \frac{\varepsilon_{33}^s w(x) l}{t_p} \frac{dv(t)}{dt} \right] \quad (39)$$

Rearranging the eq.(39) leads to:

$$\frac{dv(t)}{dt} + \frac{t_p}{\varepsilon_{33}^s w(x) l R_L} v(t) = \frac{d_{31} \left(\frac{t_s}{2} + t_p \right) E_p t_p}{\varepsilon_{33}^s l} \int_{x=0}^{x=l} \frac{\partial^3 z_{rel}(x,t)}{\partial x^2 \partial t} dx \quad (40)$$

Using separation of variables technique leads to:

$$z_{rel}(x,t) = \sum_{k=1}^{\infty} w_k(x) q_k(t) \quad (41)$$

Using eq.(41), the integral term in eq. (40) can be written as:

$$\int_{x=0}^{x=l} \frac{\partial^3 z_{rel}(x,t)}{\partial x^2 \partial t} dx = \sum_{k=1}^{\infty} \frac{dq_k(t)}{dt} \int_0^l \frac{d^2 w_k(x)}{dx} dx = \left. \frac{dq_k(t)}{dt} \frac{dw_k(x)}{dx} \right|_{x=l} \quad (42)$$

Simplifying eq. (40) gives the ordinary differential equation of piezoelectric energy harvester as:

$$\frac{dv(t)}{dt} + \frac{t_p}{\varepsilon_{33}^s w l R_L} v(t) = \sum_{k=1}^{\infty} \phi_k \frac{dq_k(t)}{d\tau} \quad (43)$$

where:

$$\phi_k(x) = -\frac{d_{31} E_p h_p (h_s / 2 + h_p)}{\varepsilon_{33}^s L} \left. \frac{dw_k(x)}{dx} \right|_{x=L} \quad (44)$$

Eq.(43) can be solved for $v(t)$ by multiplying the following integrating factor through differential equation in order to bring the left-hand side under a common derivative:

$$\psi(t) = e^{-t/\tau_c} \quad (45)$$

where τ_c is the circuit time constant and can be expressed by:

$$\tau_c = \frac{R_L \varepsilon_{33}^s w l}{t_p} \quad (46)$$

Combining eq.(35) and eq.(41) leads to:

$$\sum_{k=1}^{\infty} \frac{d^2}{dx^2} \left[EI(x) \frac{d^2 w_k(x)}{dx^2} \right] q_k(t) + \sum_{k=1}^{\infty} \left[\frac{d^2}{dx^2} \left[C_s I(x) \frac{d^2 w_k(x)}{dx^2} \right] + C_a \right] \frac{dq_k(t)}{dt} + m(x) \sum_{k=1}^{\infty} w_k(x) \frac{d^2 q_k(t)}{dt^2} + \frac{d^2}{dx^2} \left[\eta(x) \left[\frac{d\delta(x)}{dx} - \frac{d\delta(x-l)}{dx} \right] \right] v(t) = -m(x) + M_l \delta(x-l) \frac{\partial^2 z_b(x,t)}{\partial t^2} \quad (47)$$

Integrating eq.(47) over the length of the beam after multiplying it by $w_p(x)$ and using orthogonality condition gives the equation of motion as follows:

$$\frac{d^2 q_k(\tau)}{d\tau^2} + 2\zeta_k \omega_k \frac{dq_k(\tau)}{d\tau} + \omega_k^2 q_k(\tau) + \lambda_k v(\tau) = - \left[\int_0^l w_k(x) m(x) dx + M_l w_k(l) \right] \frac{d^2 w_b(x)}{dt^2} \quad (48)$$

where λ_k represents the modal coupling term and is dependent on the cantilever shape. For a rectangular cantilever it can be obtained as:

$$\lambda_k = \eta \left. \frac{dw_k(x)}{dx} \right|_{x=l} \quad (49)$$

For an exponentially tapered cantilever, the modal coupling term is expressed as below:

$$\lambda_k = \int_0^l w_k(x) \frac{d^2 \eta(x)}{dx^2} dx + \left. \frac{d(w_k(x)\eta(x))}{dx} \right|_{x=0} - \left. \frac{d(w_k(x)\eta(x))}{dx} \right|_{x=l} + 2 \left(w_k(0) \left. \frac{d\eta(x)}{dx} \right|_{x=0} - w_k(l) \left. \frac{d\eta(x)}{dx} \right|_{x=l} \right) \quad (50)$$

Modal damping ratio can be estimated using half power bandwidth method or based on the motion decay in viscous damping. If beam oscillation is harmonic in time, base motion, output voltage and electrical charge can be written as $z_b = Y_0 e^{i\omega t}$,

$v(t) = V_0 e^{i\omega t}$ and $q_k(t) = Q_k e^{i\omega t}$ respectively. Thus $q_k(t)$ becomes:

$$q_k(t) = \frac{\left[m\omega^2 Y_0 \int_0^l w_k(x) dx - \lambda_k V_0 \right] e^{i\omega t}}{\omega_k^2 - \omega^2 + 2i\zeta_k \omega_k \omega} \quad (51)$$

where i is the imaginary number sign and ω is the driving frequency. Also substituting $v(t) = V_0 e^{i\omega t}$ in eq.(43) can lead to:

$$\left(\frac{1+i\omega\tau_c}{\tau_c}\right)V_0e^{i\omega t} = \sum_{k=1}^{\infty}\phi_k \frac{dq_k(t)}{dt} \quad (52)$$

Differentiating eq.(51) and substituting in eq.(52) can lead to the voltage amplitude across the resistance:

$$\left(\frac{1+i\omega\tau_c}{\tau_c}\right)V_0e^{i\omega t} = \sum_{k=1}^{\infty}\phi_k \frac{i\omega \left[m\omega^2 Y_0 \int_0^l w_k(x)dx - \lambda_k V_0 \right] e^{i\omega t}}{\omega_k^2 - \omega^2 + 2i\zeta_k \omega_k \omega} \quad (53)$$

So the ratio of the output voltage to the base acceleration or voltage FRF is as below:

$$\frac{v(t)}{\omega^2 Y_0 e^{i\omega t}} = \frac{\sum_{k=1}^{\infty} \frac{im\omega\phi_k \left(\int_0^l w_k(x)dx \right)}{\omega_k^2 - \omega^2 + 2i\zeta_k \omega_k \omega}}{\left(\sum_{k=1}^{\infty} \frac{i\omega\lambda_k\phi_k}{\omega_k^2 - \omega^2 + 2i\zeta_k \omega_k \omega} \right) + \frac{1+i\omega\tau_c}{\tau_c}} \quad (54)$$

It is notable that for tapered cantilevers, some modifications in the area moment of inertia, $I(x)$, and the width function, $w(x)$, must be considered. In this case, the width function of beam shape is defined as [9]:

$$w(x) = ratio \times w(0) + \frac{w(0)(1-ratio)}{l} l - x \quad (55)$$

4. Finite element analysis

In order to investigate the accuracy of (21), finite element analysis is done in ABAQUS 6.14 software.

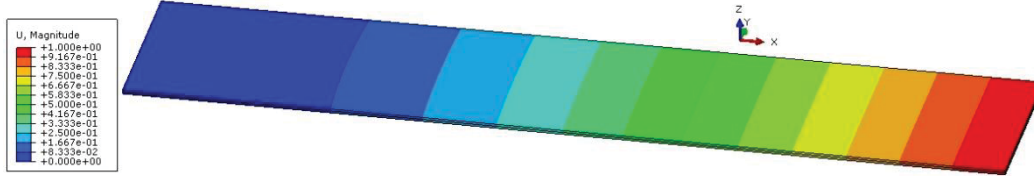


Figure 6 Deformed shaped for the first vibration mode of unimorph rectangular piezoelectric cantilever

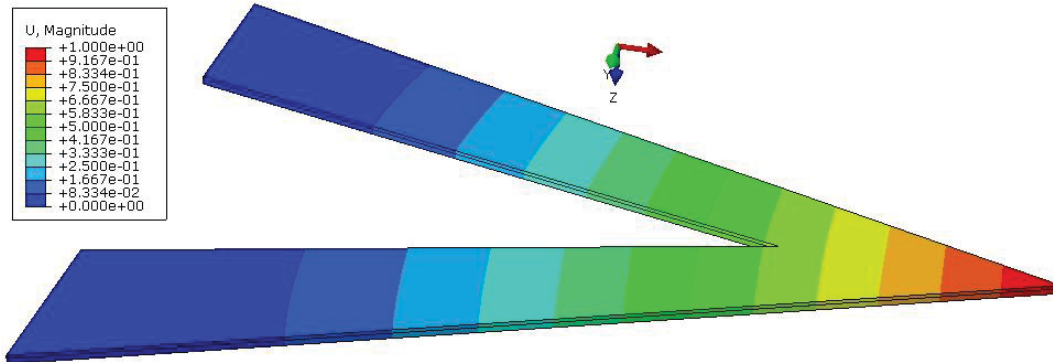


Figure 7 Deformed shaped for the first vibration mode of trapezoidal V-shaped cantilever ($w_2=0$ mm and $l_0=70$ mm)

Consider a unimorph rectangular cantilever, assuming $\rho_s=8740\text{kg/m}^3$, $\rho_p=7800\text{kg/m}^3$, $E_s=9.7 \times 10^{10}\text{Pa}$, $E_p=6.6 \times 10^{10}\text{Pa}$, $t_s=1\text{mm}$, $t_p=1\text{mm}$, $w_l=80\text{mm}$ and $l_l=400\text{mm}$. The simulated shape is shown in Figure 6 and the obtained frequency in ABAQUS is 6.30 Hz.

Also a set of unimorph trapezoidal V-shaped cantilever beams with different forms, assuming, $\rho_s=8740\text{kg/m}^3$, $\rho_p=7800\text{kg/m}^3$, $E_s=9.7 \times 10^{10}\text{Pa}$, $E_p=6.6 \times 10^{10}\text{Pa}$, $t_s=0.6\text{mm}$, $t_p=0.4\text{mm}$, $w_0=40\text{mm}$, $w_l=80\text{mm}$, $l_l=100\text{mm}$ and altering w_2 and l_0 are simulated. When $w_2=0\text{mm}$ and $l_0=70\text{mm}$, the simulated shape is shown in Figure 7 and the natural frequency is almost 76 Hz.

The relative error δ is introduced to compare the results using the obtained formulas with the corresponding finite element simulation.

$$\delta = \frac{f - f'}{f} \quad (56)$$

where f refers to the calculation results with (16) and (21), and f' refers to finite element simulation results with ABAQUS 6.14 analysis. The frequency calculation for a rectangular shape, according to (16) is 6.34 Hz and the corresponding simulation result with ABAQUS is 6.30 Hz. Hence the relative error is only 0.66% and an excellent agreement is obtained between the calculation results and the finite element simulation results, yielding negligible relative error. The calculations according to (21) and the corresponding finite element simulation results with ABAQUS 6.14 when the w_2 is variable, are listed in Table 1.

Table 1 analytical and the simulation results of the resonant frequencies of unimorph trapezoidal V-shaped cantilever beams (w_2 is variable and $l_0=70\text{mm}$)

$w_2(\text{mm})$	$f(\text{Hz})$	$f'(\text{Hz})$	$\delta\%$
0	80.90	76.09	5.95 %
10	64.11	62.73	2.15 %
20	55.70	54.83	1.56 %
30	50.52	50.71	-0.38 %
40	46.97	46.86	0.23 %
50	44.35	44.69	-0.77 %
60	42.34	42.68	-0.80 %
70	40.74	41.19	-1.10 %
80	39.44	40.22	-1.98 %

In Figure 8, it can be seen that how the frequency (f and f') varies with w_2 . By increasing the cantilever tip width (w_2), the frequency decreases.

It can be seen from Table 1 and Figure 8 that, a good agreement is obtained between the analytical results and the simulation results. So the relative error is slight (less than 6%).

The calculations according to (21) and the corresponding simulation results with ABAQUS 6.14 when the l_0 is variable, are listed in Table 2.

In Figure 9, the variations of the frequency (f and f') against l_0 is shown. In a certain length, the frequency reaches its minimum value.

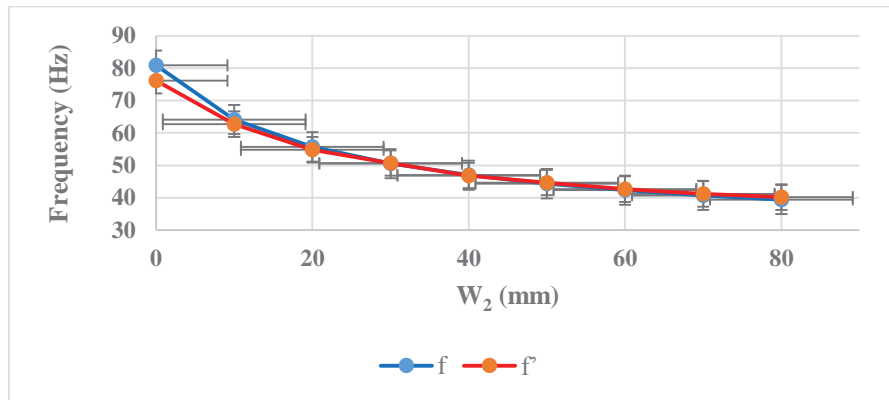


Figure 8 frequency variations against cantilever tip width

Table 2 analytical and simulation results of the resonant frequencies of unimorph trapezoidal V-shaped cantilevers (l_0 is variable and $w_2=40\text{mm}$)

$l_0(\text{mm})$	$f(\text{Hz})$	$f'(\text{Hz})$	δ
0	58.26	60.61	-4.03 %
10	55.9	57.2	-2.33 %
20	53.75	54.77	-1.90 %
30	51.83	51.38	0.87 %
40	50.17	50.86	-1.38 %
50	48.78	48.72	0.12 %
60	47.7	48.14	-0.92 %
70	46.97	46.86	0.23 %
80	46.63	47.05	-0.90 %
90	46.71	48.13	-3.04%

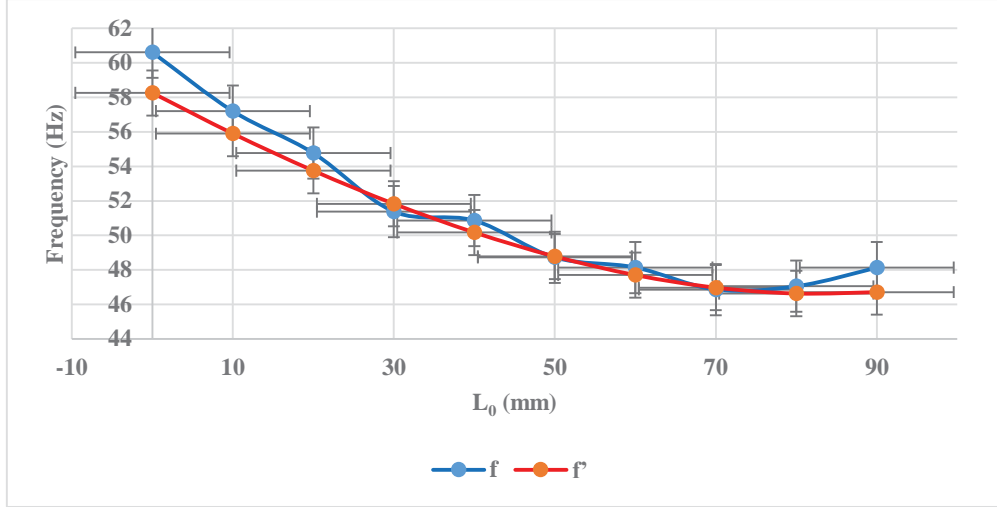


Figure 9 frequency variations against cantilever beam length

It can be seen from Table 2 and Figure 9 that, a good agreement is obtained between the analytical results and the simulation results. Hence a little relative error occurs (less than 4.04%). When $l_0=0$ the relative error is maximum and the V-shaped cantilever will be transformed to the simple tapered beam. In other cases, the agreement between simulation results and analytical results is better.

Due to the above, in the same condition in length l_1 , width w_1 , thickness t_1 and t_2 and material properties E_1 , E_2 , ρ_1 and ρ_2 , triangular tapered cantilever beam has the highest resonant frequency and therefore maximum sensitivity as obtained in [13]. It is notable that the triangular tapered cantilever is a special kind of V-shaped cantilever with $w_0=w_2=0$.

The highest resonant frequency is achieved by substituting $a=c=0$ into (21):

$$\begin{aligned}
 f_{top} &= \frac{\sqrt{210}}{\pi l_1^2} \sqrt{\frac{E_s t_s^3 + 2E_p t_p^3 + \frac{E_p t_p t_s^2}{2} + E_p t_s t_p^2}{\rho_s t_s + 2\rho_p t_p}} g(0, b, 0) \\
 &= \frac{\sqrt{210}}{\pi l_1^2} \sqrt{\frac{E_s t_s^3 + 2E_p t_p^3 + \frac{E_p t_p t_s^2}{2} + E_p t_s t_p^2}{\rho_s t_s + 2\rho_p t_p}} \frac{\sqrt{3}}{7} \\
 &= \frac{\sqrt{52.5}}{7\pi l_1^2} \sqrt{\frac{E_s t_s^3 + 8E_p t_p^3 + 6E_p t_p t_s^2 + 12E_p t_s t_p^2}{\rho_s t_s + 2\rho_p t_p}} \\
 &\approx \frac{0.3295}{l_1^2} \sqrt{\frac{E_s t_s^3 + 8E_p t_p^3 + 6E_p t_p t_s^2 + 12E_p t_s t_p^2}{\rho_s t_s + 2\rho_p t_p}}
 \end{aligned} \quad (57)$$

As can be seen from the derived equation, the resonant frequency of a unimorph tapered cantilever beam ($l_0=0$) is not dependent on its width w_1 . It should be noted that for a unimorph tapered cantilever beam, when w_1 increases, while other parameters are fixed, the resonant frequency does not change. By comparing (16) and (57), the resonant frequency ratio of unimorph

triangular tapered cantilever and unimorph rectangular one is obtained:

$$\frac{f_{top}}{f_{rect}} = \frac{0.3295}{l_1^2} \sqrt{\frac{(E_s t_s^3 + 8E_p t_p^3 + 6E_p t_p t_s^2 + 12E_p t_s t_p^2)}{\rho_s t_s + 2\rho_p t_p}} = 2.0104 > 2 \quad (58)$$

Hence, the unimorph tapered cantilever beams are more sensitive than rectangular ones to vibrations, because tapered cantilevers can lead to higher resonant frequency and so higher sensitivity.

To validate the obtained formula in eq.(54), finite element simulation is carried out for different beams which consist of a brass substrate layer under a PZT-5A layer with $\rho_s=8490\text{kg/m}^3$, $\rho_p=7750\text{kg/m}^3$, $E_s=9.7 \times 10^{10}\text{Pa}$, $E_p=5.1 \times 10^{10}\text{Pa}$ and different geometrical parameters described in Table 3.

The simulated shape for a rectangular beam with $l_0=0\text{mm}$, $l_1=28.6\text{mm}$, $w_0=0\text{mm}$, $w_1=3.175\text{mm}$, $w_2=3.175\text{mm}$, $t_s=0.132\text{mm}$ and $t_p=0.188\text{mm}$ is shown in Figure 10. It can be seen that the simulated output voltage is 6.57V. Also the other geometries in Table 3 are analyzed using FEM and the results are shown in Figure 11 and Figure 12.

The cross section of voltage distribution in the piezoelectric layer of the simulated unimorph trapezoidal cantilever beam with the same volume, is shown in Figure 13.

The calculation according to (54) and the corresponding simulation results with ABAQUS, are listed in Table 4.

Table 3 Geometrical parameters of the models

Cantilever shape	Volume (mm ³)	Length (mm)	w ₁ (mm)	w ₂ (mm)	Piezoelectric thickness (mm)	Substrate thickness (mm)
Rectangular	29.06	28.6	3.175	3.175	0.188	0.132
Trapezoid with low volume	23.81	28.6	3.175	2.028	0.188	0.132
Trapezoid	29.06	40.8	3.175	1.270	0.188	0.132

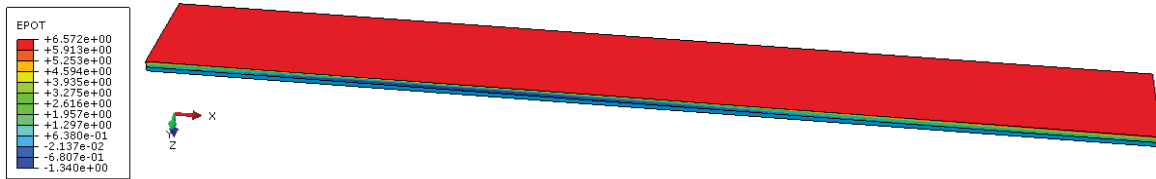


Figure 10 Output voltage of simulated unimorph rectangular piezoelectric cantilever

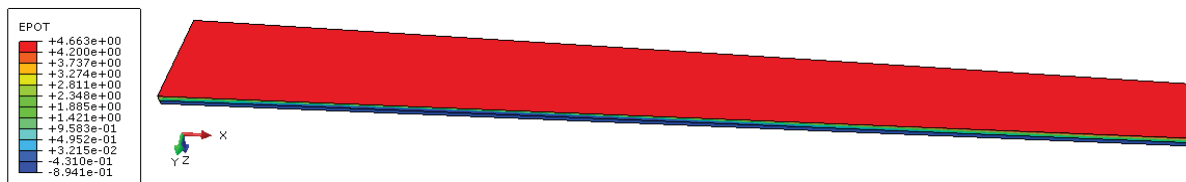


Figure 11 Output voltage of simulated trapezoidal unimorph piezoelectric cantilever with low volume

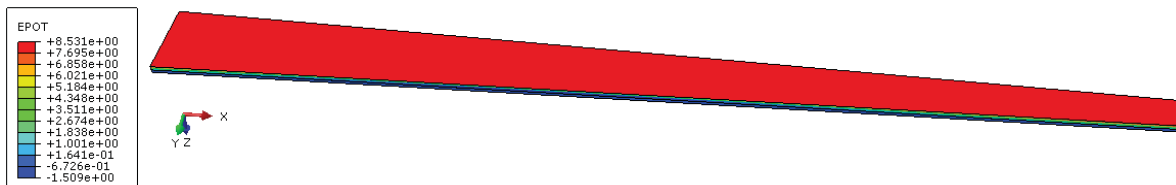


Figure 12 Output voltage of simulated unimorph trapezoidal piezoelectric cantilever with same volume

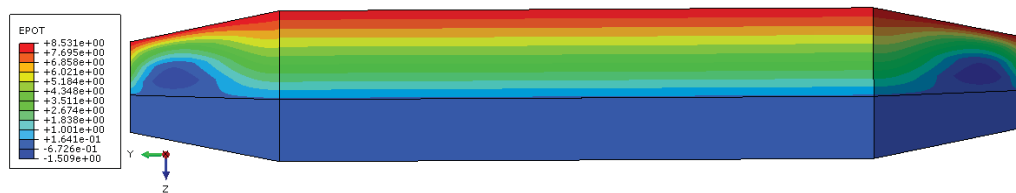


Figure 13 voltage distribution in the unimorph trapezoidal piezoelectric cantilever

Table 4 Voltage output of different harvester shapes with different calculation methods (V)

	Rectangular	Trapezoid with low volume	Trapezoid
FE simulation	6.57	4.66	8.53
Calculation results	6.32	4.86	8.22

Table 4 indicates good agreement between simulation and theoretical results, so that the difference between the results is negligible (less than 5%). It can be seen that the trapezoidal geometry leads to more power density in piezoelectric material.

As mentioned before in [13] for bimorph cantilevers, as the beam becomes truncated, the

generated voltage per unit mass and hence the power density, increases and it is in maximum value for a triangular beam when the width-ratio (w_2/w_1) becomes zero. In a general analysis, strain distribution of a triangular cantilever is more uniform than a rectangular one. In other words, a triangular geometry is more efficient than a rectangular one. The strain distribution of different shapes with the same length,

width and thickness under similar tip displacement is shown in Figure 14. As can be seen in Figure 14-(a), in the rectangular cantilever, the maximum strain is located in a small area. The strain distribution in the Figure 14-(b) is better than Figure 14-(a). It can be seen from Figure 14-(c) that the strain distribution of a semi-triangular cantilever energy harvester is almost uniform and close to its maximum value.

5. Conclusion

This paper deduces a highly precise explicit formula for approximating the fundamental resonant frequency of unimorph trapezoidal V-shaped cantilevers based on the Rayleigh method. The analytical results are in a good agreement with the finite element simulation results and the relative error is negligible. In addition to determining the resonant frequency of unimorph trapezoidal V-shaped cantilevers of any material and geometrical properties, the presented resonant frequency formula can be used to design and optimization of unimorph trapezoidal V-shaped cantilever energy harvesters which are considered among the best and highest performance. The shape of the cantilever in the first mode of vibration is not exactly the same as static deflection profile. So the natural frequency estimates are slightly different from

the simulation values. The formula presented for calculating natural frequency of unimorph tapered cantilevers, is a simple, relatively precise and practical formula for making some determination. Also the output voltage of unimorph piezoelectric cantilever beam is formulated and the formula is validated by finite element simulation results. Simulation results demonstrate that under the same loading, material and geometrical conditions, triangular cantilever beams are more efficient than other trapezoidal and rectangular ones. A family of beam shapes ranging from rectangular beams to triangular beams in terms of resonant frequency, output voltage and efficiency have been investigated. It turns out that the shape can have a great effect on the output voltage and therefore maximum output power density. It can be concluded that the deformation, strain and voltage of a triangular vibration energy harvester is more than those of a rectangular or trapezoidal one. Combining the triangular shape energy harvesters and the multi-modal energy harvester designs, can create the most power density and so optimized schemes. The results of this study can provide design guidance toward fabricating high power piezoelectric energy harvesters.

Conflict of Interest: The authors declare that they have no conflict of interest.

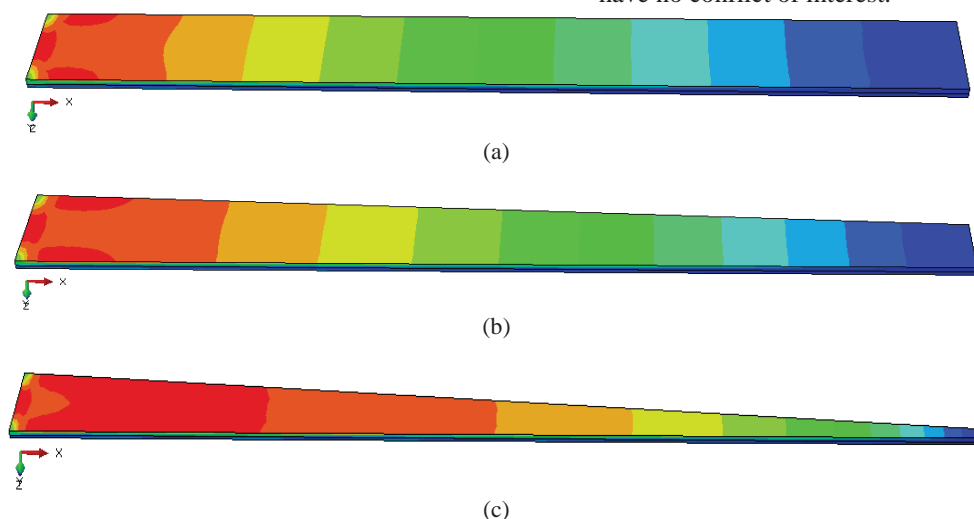


Figure 14 Strain distributions of three different piezoelectric vibrators

References

- [1] S. Priya and D. J. Inman, *Energy harvesting technologies* vol. 21: Springer, 2009.
- [2] J. Baker, S. Roundy, P. Wright, Alternative geometries for increasing power density in vibration energy scavenging for wireless sensor networks, in *Proceeding of*.
- [3] A. D. Dimarogonas, 1996, *Vibration for engineers*, Prentice Hall,
- [4] T. A. Anderson, D. W. Sexton, A vibration energy harvesting sensor platform for increased industrial efficiency, in *Proceeding of*, International Society for Optics and Photonics, pp. 61741Y-61741Y-9.
- [5] S. P. Beeby, M. J. Tudor, N. White, Energy harvesting vibration sources for microsystems applications, *Measurement science and technology*, Vol. 17, No. 12, pp. R175, 2006.
- [6] A. Erturk, D. J. Inman, A distributed parameter electromechanical model for cantilevered piezoelectric energy harvesters,

- Journal of vibration and acoustics*, Vol. 130, No. 4, pp. 041002, 2008.
- [7] S. Matova, M. Renaud, M. Jambunathan, M. Goedbloed, R. Van Schaijk, Effect of length/width ratio of tapered beams on the performance of piezoelectric energy harvesters, *Smart Materials and Structures*, Vol. 22, No. 7, pp. 075015, 2013.
- [8] N. Siddiqui, UNDERSTANDING EFFECTS OF TAPERING CANTILEVERED PIEZOELECTRIC BIMORPHS FOR ENERGY HARVESTING FROM VIBRATIONS, 2014.
- [9] A. G. Muthalif, N. D. Nordin, Optimal piezoelectric beam shape for single and broadband vibration energy harvesting: Modeling, simulation and experimental results, *Mechanical Systems and Signal Processing*, Vol. 54, pp. 417-426, 2015.
- [10] R. Hosseini, M. Hamed, An investigation into resonant frequency of trapezoidal V-shaped cantilever piezoelectric energy harvester, *Microsystem Technologies*, Vol. 22, No. 5, pp. 1127-1134, 2016.
- [11] R. Hosseini, M. Hamed, An Investigation into Resonant Frequency of Triangular V-Shaped Cantilever Piezoelectric Vibration Energy Harvester, *Journal of Solid Mechanics*, Vol. 8, No. 3, pp. 560-567, 2016.
- [12] K. Yang, Z. Li, Y. Jing, D. Chen, T. Ye, Research on the resonant frequency formula of V-shaped cantilevers, in *Proceeding of*, 59-62.
- [13] R. Hosseini, M. Hamed, Improvements in energy harvesting capabilities by using different shapes of piezoelectric bimorphs, *Journal of Micromechanics and Microengineering*, Vol. 25, No. 12, 2015.
- [14] R. Hosseini, M. Hamed, Study of the Resonant Frequency of Unimorph Triangular V-shaped Piezoelectric Cantilever Energy Harvester, *International Journal of Advanced Design and Manufacturing Technology*, Vol. 8, No. 4, 2015.
- [15] J. Lubliner, P. Papadopoulos, 2013, *Introduction to Solid Mechanics: An Integrated Approach*, Springer Science & Business Media,
- [16] C. W. De Silva, 2006, *Vibration: fundamentals and practice*, CRC press,
- [17] S. S. Rao, 2007, *Vibration of continuous systems*, John Wiley & Sons,
- [18] R. Hosseini, M. Hamed, Resonant frequency of bimorph triangular V-shaped piezoelectric cantilever energy harvester, *Journal of Computational and Applied Research in Mechanical Engineering*, Vol. 6, No. 1, pp. 65-73, 2016.
- [19] A. Erturk, D. J. Inman, 2011, *Piezoelectric energy harvesting*, John Wiley & Sons,